Kinetic energy release distributions in the Coulomb explosion of N_2 molecules induced by fast, highly-charged-ion impact

B. Siegmann,[1] U. Werner,[1] R. Mann,[2] N. M. Kabachnik,[1,*] and H. O. Lutz[1]
[1]*Fakultät für Physik, Universität Bielefeld, D-33615 Bielefeld, Germany*
[2]*Gesellschaft für Schwerionenforschung (GSI), D-64291 Darmstadt, Germany*
(Received 15 February 2000; published 20 July 2000)

The dissociation of molecular ions $(N_2)^{q+}$ produced by 4.7 MeV/amu $Bi^{57+,25+}$ and 5.9 MeV/amu $Xe^{43+,18+}$ ion impact on N_2 has been studied using the coincidence technique with a position- and time-sensitive multiparticle detector. The kinetic energy release distributions for all observed ion pairs $N^{q_1+}+N^{q_2+}$ are measured. Analysis of the distributions is made with emphasis on the highly charged-molecular ions, $q>3$. In these cases the most probable total kinetic energy of the two fragments is quite well described by the Coulomb explosion model for point charges, while the measured width of the distributions is much larger than that predicted by this simplified model. We therefore suggest a more elaborate model of Coulomb fragmentation based on a statistical description of the individual potential energy curves of the molecular ion. This enables us to describe both the position and the width of the kinetic energy release distributions. We suggest that the main cause of the large width of the distributions for the high q values is the spread of the potential energy curves at the equilibrium internuclear distance; this is mainly due to the dispersion interaction arising from the mutual polarization of the atomic ions.

PACS number(s): 34.50.Gb, 34.10.+x

I. INTRODUCTION

The dissociation of multiply charged molecular ions into charged fragments, often referred to as Coulomb explosion, has been subject of intensive investigation in the last decade. One of the most effective means for creating multiply charged molecular ions is an ion-molecule collision. In combination with the coincident detection of the molecular fragments, it provides the unique possibility of a kinematically complete study of the dissociation dynamics of highly excited and highly charged molecular ions. Using this method the Coulomb fragmentation of simple molecules has been studied for light (H^+,He^+) and heavy ion impact at low [1–9], medium [4,10,11], and high [9,12–21] velocities. Only at very low velocities the fragmentation process is significantly influenced by the presence of the passing projectile [8,9]. At sufficiently high velocities the characteristic fragmentation times (around 10 fs) are much longer than the collision time, and the kinetic energy distribution of the fragments directly reflects the properties of the excited molecular states of the multiply ionized molecule. This is the condition under which we shall further discuss the fragmentation process. For a diatomic molecular ion $(AB)^{q+}$ the simple picture of the Coulomb explosion suggests that the total kinetic energy of the two fragments A^{q_1+} and B^{q_2+} $(q=q_1+q_2)$ is equal to the Coulomb potential energy q_1q_2/R_e of pointlike charges at the equilibrium distance R_e (atomic units are used throughout unless otherwise indicated). Numerous experimental data confirm that the most probable kinetic energy released in the fragmentation is approximately described by this simple model (see, for example, Refs. [4,10,17,20]). On the other hand it is well known that the shape and the width of the total kinetic energy release (KER) distribution cannot be explained by the Coulombic model [4,9,11,13,17,20,21]. It is generally believed that the observed structure of the KER spectra is determined by particular molecular states which are populated in the collision. This is consistent with the known fact that at small and medium collision energies the KER distributions depend on the projectile type and velocity [2–4,6,18]. This may be interpreted in such a way that the cross sections for transitions to particular states vary with the projectile energy, thus resulting in a variation of the KER spectra. Several successful attempts to theoretically describe the KER distributions starting from *ab initio* calculations of molecular potential energy curves for some lowest states of doubly or triply charged molecular ions [2,6,9,11,12,22] confirm this idea. Another interpretation based on the classical trajectory Monte Carlo model has been suggested recently [8] for molecular fragmentation by slow highly charged ion impact. The most dramatic manifestation of the non-Coulombic character of the dissociation of multiply charged molecular ions is the width of the KER distribution. In a simple Coulombic model the width is determined by the reflection of the ground state probability density off the Coulomb potential curve [1]. The resulting KER distribution is approximately Gaussian with a width of a few eV [17,21] which is much less than the observed width of up to 100–120 eV for higher degrees of ionization.

In the experiment to be described the projectile velocity is much larger than the velocity of almost all electrons of the target molecule ($v\sim 15v_0$, where v_0 is the Bohr velocity) thus the ionization process is highly nonadiabatic, and the direct ionization of target electrons dominates. For the further discussion it is convenient to characterize the interaction strength by the so-called Sommerfeld parameter $\kappa=Q/v$ where Q is the projectile charge and v its velocity. At small $\kappa\ll 1$ the target is only slightly perturbed by the projectile, and first order perturbation theories are applicable. In this regime, the ionization probabilities and the resulting KER

*On a leave of absence from the Institute of Nuclear Physics, Moscow State University, Moscow 119899, Russian Federation.

distributions are found to depend strongly on the projectile charge and velocity. In contrast, in the strong interaction regime ($\kappa>1$) the characteristics of the fragmentation process, i.e., the shape and width of the KER distributions, reveal a tendency to saturate [18,20,21]. Most earlier experiments with fast ion beams have been carried out in the range $\kappa<1$. Only very recently first data became available for molecular fragmentation induced by fast very highly charged ions of Xe^{44+}($\kappa=2.7$) [20] and Bi^{57+}($\kappa=4.2$) [21].

In the present paper we discuss fast collisions in the strong interaction regime $Q>v\gg v_0$, so that $\kappa>1$. We concentrate on the dissociative ionization of the N_2 molecule in this regime, in particular on the interpretation of the KER distributions for the highly charged molecular $(N_2)^{q+}$ ions ($q\geqslant 4$). Analysis of lower charge states is published separately [22]. Using highly charged Bi and Xe projectile ions at energies of 4.7 and 5.9 MeV/amu we explore the region of $\kappa=1.2-4.2$. One of our goals is to study the projectile velocity and projectile charge state dependence of the kinetic energy release.

In Sec. II a brief description of the experiment and the data evaluation procedure will be given. In Sec. III we present and discuss the experimental data. Section IV presents a semiphenomenological model based on a statistical approach. It describes the gross parameters of the spectra, namely the position of the maximum and the width of the KER distribution. The model predictions are compared with the experimental data. Some conclusions and perspectives are outlined in the final Sec. V.

II. EXPERIMENT AND ITS ANALYSIS

The experiment has been performed using the highly charged ion beam of the UNILAC accelerator at the GSI Darmstadt. Bi^{25+} and Bi^{57+} ions with an energy of 4.7 MeV/amu and Xe^{18+} and Xe^{43+} ions with an energy of 5.9 MeV/amu have been injected into a dilute N_2 gaseous target. Details of the experimental setup can be found elsewhere [4,23]. Here we will give only brief description of the experiment and of the data evaluation procedure.

The collimated MeV/amu projectile beam interacts with the N_2 gas target. The slow N^{q+} ions and electrons generated in the collision process are separated by a homogeneous electric field of 160–333 V/cm perpendicular to the detector plane. Electrons are detected in a channeltron at one side of the interaction region; positive ions are accelerated towards the time- and position sensitive multiparticle detector at the other side which is based on microchannel plates in combination with a crossed-wire anode structure [23]. After passing a field-free time-of-flight region the ions are postaccelerated to a few keV to increase the detection efficiency of the channelplates. The detector system is triggered by the first electron registered by the channeltron. For each positive fragment the position (x_i,y_i) on the detector and the time of flight t_i relative to the start electron are recorded. From these data the initial velocity vectors of the fragment ions can be determined by the use of classical mechanics.

Calculations show that the fragment velocities reach their asymptotic values $\vec{v}_{0,i}$ in a time less than 1 ps which is negligible in comparison to the total flight time of about 1 μs. Therefore it is justified to simplify the computation of trajectories assuming that they already start with their final velocity $\vec{v}_{0,i}$. The time of flight is then determined by the initial velocity component v_{0z} (along the spectrometer axis) and the detector geometry and the applied electric fields. If m/q is known for a particular fragment the initial velocity v_{0z} can be derived from the measured flight time t_i by solving $t(v_{0z})=t_i$ for v_{0z} either by numerical methods or more practical by using a look-up table. The initial velocity components (v_{0x},v_{0y}) follow from the measured position (x_i,y_i) on the detector as

$$v_{0x,i}=\frac{x_i-x_0}{t_i} \quad \text{and} \quad v_{0y,i}=\frac{y_i-y_0}{t_i}, \tag{1}$$

where (x_0,y_0,z_0) is the locus of fragmentation, i.e., the interaction point. In principle, the kinematic analysis requires a precise knowledge of (x_0,y_0,z_0). The initial z position z_0 is well determined due to the good collimation of the projectile beam, whereas the finite extension of the gas target along the projectile beam results in a rather uncertain knowledge of at least one of the remaining start coordinates. (Recent experiments using the elaborate COLTRIM technique [24] avoid this problem; unfortunately it is limited to simple targets as He and H_2.) Therefore we restrict our data analysis to those events, where both fragments are detected in coincidence. Provided the momentum is conserved among the fragments, the initial start position may be computed from the measured positions, and the kinetic energy release as well as the initial orientation of the molecular axis may be derived for each correlated fragment pair. (We note that this assumption may be problematic in certain situations, such as, e.g., in the case of very slow collisions where the projectile is still present during the dissociation process. In the fast collisions considered here the momentum transfer is believed to be small in the vast majority of collisions.)

The obtained energy resolution does not only depend on the spectrometer parameters (e.g., geometry and fields), it is also strongly influenced by the orientation of the N_2 molecular axis relative to the detector axis: a dissociating N_2 aligned along this axis would result in two fragments hitting the detector at the same position at different times, whereas a molecule oriented perpendicular to the axis would result in fragments hitting at the same time at different positions. Consequently, in the former case the energy resolution is determined by the time resolution, and by the position resolution in the latter case. In general both resolutions will contribute in a nontrivial way. Furthermore the discrete position and time values complicate an analytical treatment.

To estimate the influence of the detector on the measured energy distributions we simulated the fragmentation process taking into account all known experimental parameters. Starting from a ''known'' initial kinetic energy distribution and an isotropic orientation of the molecular N_2 axis a random sample of fragmenting molecules was generated by Monte Carlo techniques. The locus of fragmentation was chosen randomly inside the intersection of the gas target and the projectile beam. For each ''fragmenting molecule'' the

fragment trajectories inside the spectrometer were computed. The fragments were ''detected'' by a simulated detector taking into account all known properties of the system used in the experiment. Especially the finite detector size, position and time resolution and the electronic characteristics were accurately modeled. A simulated event therefore results in data sets of position and time channels. These data were analyzed using the same techniques as applied to the measured data.

These simulations were carried out for each of the observed reaction channels $N^{q_1+}+N^{q_2+}$. Since most of the measured spectra may be described approximately by a Gaussian the initial energy distributions were chosen as Gaussians with a full width at half maximum (FWHM) similar to that of the measured spectra. The simulations show that the main effect of the detector is an increase of the FWHM by 2–5 %. Furthermore, the calculations show that in case of a separation field of 333 V/cm all considered charge states were detected with a relative efficiency (neglecting the quantum efficiency of the channel plates) of at least 90%. In case of a field strength of 160 V/cm major losses occurred if one of the charges exceeded 2.

The present setup allows the separation and simultaneous measurement of all reaction channels which result in at least one electron and one or two positive fragments. The applied separation field is sufficiently large to nearly establish a 4π detector, i.e., for the kinetic energy releases occurring in the dissociation of $N^{q_1+}+N^{q_2+}$ (with $q_1,q_2\leqslant 5$) fragments are detected independent of their initial emission direction. In particular the multiparticle detector is capable of resolving particles which arrive ''at the same time'' at different positions; therefore the system is also sensitive to dissociations into the plane parallel to the detector anode. The experiment was performed under conditions guaranteeing that at most one fragmentation occurred during each active time window of the detector.

III. RESULTS AND DISCUSSION

Some examples of KER distributions are presented in Fig. 1; for further spectra we refer to Ref. [22]. All measured spectra with the exception of the spectrum for $q=2$ ($N^+ + N^+$) have a simple shape with one maximum. In some cases the existence of unresolved structure may be suggested [see, for example, Figs. 1(a) and 1(d)] possibly due to the contribution of at least two groups of molecular levels, the high-energy group contributing to the tail of the distribution. However, in the absence of any theoretical justification of the predominant population of some groups of levels we refrain from any decomposition of our spectra. In contrast with the observation of Ref. [20] for CO, within the accuracy of our experiment we have not observed any pronounced statistically significant structure in the $q>2$ spectra. As observed earlier [17,20], the spectra have in many cases an asymmetric shape with a steep slope at low energies and a longer tail at the high-energy side. This is also reflected in the noticeable difference between the average kinetic energy release E_{av} and the most probable total kinetic energy of the fragments E_m. Both these values together with the full width at half maximum (FWHM) for all measured spectra are presented in Tables I and II. We note here that the results labeled as Xe^{43+} were obatained, in fact, with the ion beam containing other charge fractions of Xe ions. In these cases, the charge state distribution had a maximum around $Q=43$ with main components Xe^{41+} (13.5%), Xe^{42+} (18.6%), Xe^{43+} (20.2%), Xe^{44+} (16.8%), and Xe^{45+} (10.9%). In all other cases an almost pure single charge fraction was used.

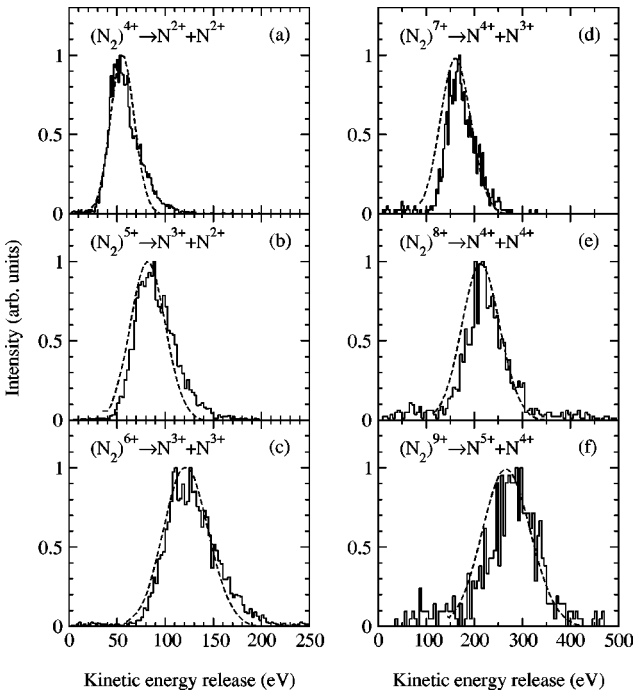

FIG. 1. Kinetic energy release distributions for several $(N_2)^{q+}$ molecular ions produced in collisions of 4.7 MeV/amu Bi^{57+} with N_2 molecules. Experimental data are shown by histograms. Broken curves represent the results of calculations in the average bunch statistical model (see text). The spectra are normalized to each other in the maximum.

It is interesting to compare the experimental KER distributions for projectiles with different charges and velocities. In a number of cases we have the possibility to compare measurements in a rather broad range of interaction strengths from $Xe^{18+}(\kappa=1.2)$ and $Bi^{25+}(\kappa=1.8)$ to $Xe^{43+}(\kappa=2.8)$ and $Bi^{57+}(\kappa=4.2)$. In Fig. 2 we show the average KER E_{av} for several fragment ion pairs as function of the Sommerfeld parameter. The kinetic energies are normalized by the corresponding values predicted by the point charge CE model. We observe a similar tendency for all ion pairs: at $\kappa\sim 1$ the average KER increases with Q/v, however, at about $\kappa\sim 3$ some saturation is achieved. The average KER is practically constant for ($\kappa>3$). In this region E_{av} is higher than predicted by the CE model for all ion pairs. However, the higher is the total charge of the fragments the closer are the values of E_{av} to the point charge CE values, what is natural since the effects determined by overlapping electron clouds diminish with decreasing number of electrons. Apparently the saturation occurs at larger κ values for larger degrees of ionization. The data presented in Fig. 2, as well as the comparison of the data in Table I and the direct comparison of

TABLE I. Parameters of the measured KER spectra for $N^{q_1+}+N^{q_2+}$ fragmentation of nitrogen molecules, induced by 5.9 MeV/amu Xe ion impact: the mean KER (E_{av}), the most probable KER (E_m), and the FWHM. The errors are shown in parenthesis. All values are in eV.

		Xe^{18+}			Xe^{43+}		
q_1	q_2	E_{av}	E_m	FWHM	E_{av}	E_m	FWHM
1	1	15.7 (0.2)	14.5	15.5 (1.0)	17.0 (0.2)	15.6	16.5 (1.2)
2	1	31.9 (0.5)	30.3	24.3 (1.0)	34.0 (0.2)	32.0	26.5 (1.0)
2	2	56.0 (0.5)	51.3	19.0 (1.0)	58.6 (0.5)	51.9	31.0 (1.0)
3	1	55.0 (1.0)	53.5	29.5 (1.0)	58.8 (0.5)	53.1	31.2 (1.0)
3	2	82.3 (0.7)	79.9	40.2 (2.0)	86.9 (0.5)	82.7	41.0 (2.0)
3	3	112.4 (1.0)	108.7	53.5 (3.0)	125.9 (1.5)	117.3	60.0 (4.0)
4	1	73.6 (1.5)	69.2	43.0 (3.0)	81.4 (1.5)	75.1	41.0 (6.0)
4	2	107.7 (1.5)	103.2	59.0 (5.0)	124.0 (1.0)	118.9	52.0 (4.0)
4	3	145.0 (2.0)	134.0	66.5 (5.0)	163.3 (1.0)	158.8	65.0 (5.0)
4	4	177.6 (2.0)	166.5	84.0 (6.0)	214.8 (1.5)	201.3	100.0 (6.0)
5	2	131.5 (3.0)	129.7	61.0 (6.0)	153.0 (2.0)	144.1	80.0 (10.0)
5	3	174.0 (4.0)	168.4	84.0 (7.0)	203.8 (2.5)	198.7	105.0 (5.0)
5	4	208.4 (3.0)	197.7	110.0 (10.0)	245.2 (3.0)	238.4	129.0 (10.0)
5	5				306.0 (5.0)	289.7	133.0 (15.0)

the spectra themselves lead to the conclusion that in fast collisions in the strong interaction region ($\kappa > 2-3$) the KER distributions are practically independent of the projectile charge and velocity. This conclusion is consistent with earlier observations [16], and it is in contrast to the situation met in the low velocity region [2,3,11].

Among the measured KER spectra there are pairs which correspond to different dissociation channels of one and the same parent molecular ion. For example, $(N_2)^{4+}$ ions can dissociate via the $N^{2+}+N^{2+}$ channel or via the $N^{3+}+N^{+}$ channel. As is reported also in [22], such KER spectra for these two channels are identical within the accuracy of our measurements [see Fig. 3(a)]. A similar resemblance is demonstrated by a pair of distributions for $q=6$: $N^{3+}+N^{3+}$ and $N^{4+}+N^{2+}$ [see Fig. 3(b)]. Although the widths of both distributions are slightly different, both maxima practically coincide. A possible explanation of the striking similarity of such KER distributions is that the dense manifolds of the potential curves corresponding to different asymptotic charge states of the fragments have multiple crossings at distances where the kinetic energy of the fragments is already determined. Therefore, due to charge exchange processes the KER spectrum in a weakly populated asymmetric channel is practically identical with the one in the corresponding strongly populated symmetric channel.

In the following we concentrate on the fragment charge dependence of the gross characteristics of the KER distributions, namely the most probable KER and the width of the KER distributions, in the cases when $q_1=q_2$ and $q_1=q_2+1$. Figure 4 shows the dependence of the most probable value of the KER E_m and the FWHM as function of the product of the fragment charges q_1q_2. The dashed curves show the prediction of the simple Coulomb explosion (CE) model for point charges. In this case the kinetic energy of the fragments would simply be $E_m=q_1q_2/R_e$, where R_e is the equilibrium internuclear distance of the neutral parent mol-

TABLE II. The same as in Table I but for 4.7 MeV/amu Bi ion impact.

		Bi^{25+}			Bi^{57+}		
q_1	q_2	E_{av}	E_m	FWHM	E_{av}	E_m	FWHM
1	1	17.7 (0.2)	14.7	17.0 (1.0)	17.9 (0.2)	15.4	16.0 (0.5)
2	1	33.6 (0.4)	30.8	26.3 (2.0)	34.6 (0.2)	32.3	25.1 (0.5)
2	2	58.2 (0.6)	53.6	28.5 (1.0)	59.0 (0.3)	54.9	29.5 (1.0)
3	1	55.3 (3.0)	53.5	29.9 (2.0)	60.0 (0.3)	55.7	29.0 (1.5)
3	2	87.8 (0.7)	84.2	42.9 (4.0)	91.0 (0.7)	87.4	43.4 (4.0)
3	3	124.4 (1.5)	119.1	52.5 (6.0)	129.3 (1.0)	124.5	55.4 (5.0)
4	2	119.5 (4.0)	116.8	51.5 (6.0)	122.3 (0.5)	121.3	52.4 (3.0)
4	3	158.5 (4.0)	156.2	68.5 (8.0)	173.0 (0.5)	169.0	55.2 (5.0)
4	4	207.0 (9.0)	185.4	107.0 (10.0)	224.5 (4.0)	220.3	84.6 (8.0)
5	4				276.5 (7.0)	282.2	117.0 (12.0)
5	5				322.0 (10.0)	338.7	122.0 (15.0)

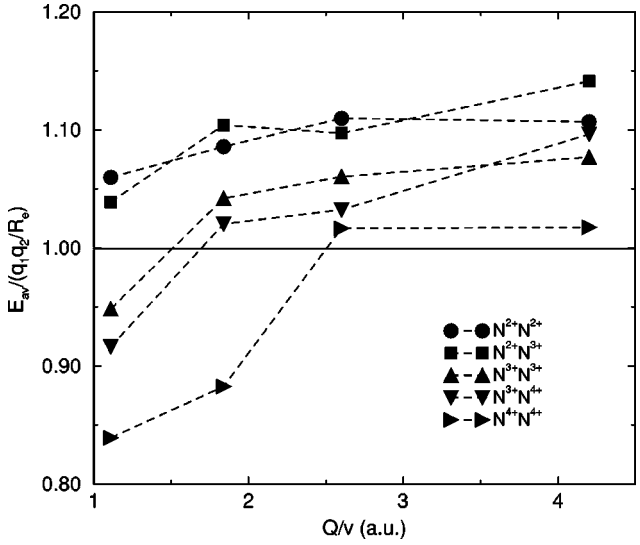

FIG. 2. The mean kinetic energy of fragments measured in the present experiment for several ion pairs, normalized to the prediction of the point charge CE model, as function of the interaction strength $\kappa = Q/v$. The lines are drawn to guide the eye.

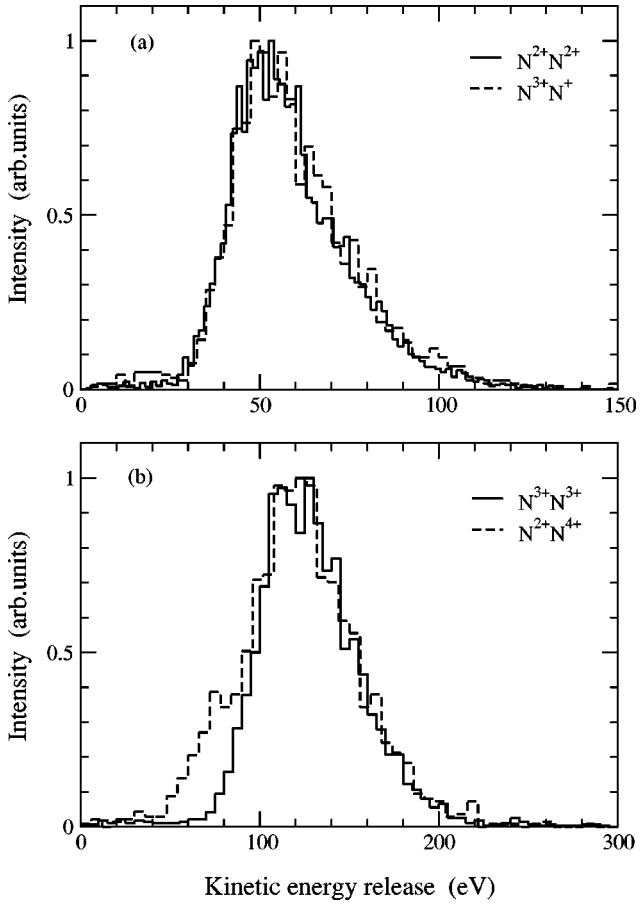

FIG. 3. A comparison of the KER distributions for nitrogen ions produced in collision of N_2 with 4.7 MeV/amu Bi^{57+} ions and observed in different dissociation channels of the molecular ions $(N_2)^{4+}$ (a) and $(N_2)^{6+}$ (b).

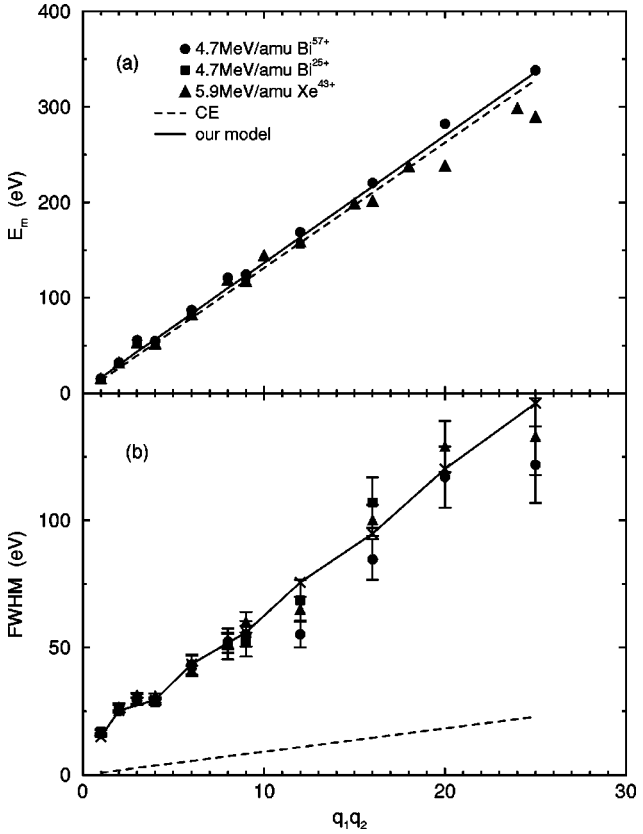

FIG. 4. The most probable total kinetic energy (a) and the FWHM (b) of the KER distributions as functions of q_1q_2 of different charge pairs. The experimental data are obtained with 4.7 MeV/amu Bi^{57+} (dots), Bi^{25+} (squares) and 5.9 MeV/amu Xe^{43+} (triangles). Dashed curves show the prediction of the simple point-charge CE model. Crosses connected by solid lines show the results of calculations in our model.

ecule, which in N_2 is $R_e = 2.07$ a.u. The width of the KER distribution can be determined by reflecting the molecular ground state probability density off the Coulomb potential curve. Since the Franck-Condon region is rather narrow, the width can be estimated to first approximation as

$$W_c \approx -\frac{dU}{dR}(R_e)\,\delta R = \frac{q_1 q_2}{R_e^2}\,\delta R, \tag{2}$$

where δR is the width of the molecular ground state which in the case of N_2 is $\delta R = 0.144$ a.u. The dashed curve in Fig. 4(b) represents Eq. (2). Clearly, the simple CE model predicts rather accurately the position of the spectral maximum. However, it strongly underestimates the width, in agreement with earlier measurements both for N_2 [4,21] and CO molecules [17]. It is well understood that the reason for this discrepancy is found in the ensemble of non-Coulombic potential energy curves which characterize the dissociating molecular ion: the large width of the KER spectra indicates that numerous potential energy curves exist which are steeper or shallower than the Coulomb curve in the Franck-Condon region and which are effectively populated in the collision. The width associated with any individual curve constitutes

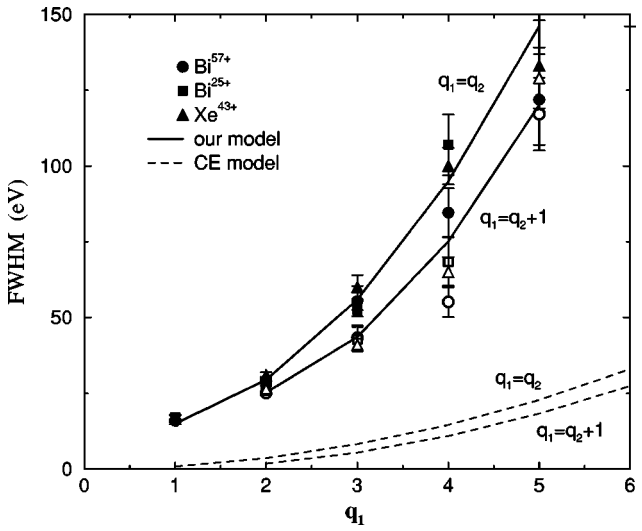

FIG. 5. The FWHM of the KER distributions presented as a function of the charge of one of the fragments (q_1). Experimental data are the same as in Fig. 4. Filled symbols correspond to the case $q_1=q_2$, open symbols correspond to $q_1=q_2+1$. Theoretical results are connected by solid lines: our model; dashed lines: point-charge CE model.

only a small fraction of the total width. The potential curves are spread in energy and the total spectrum is a sum of the contributions of many individual curves. Until now there were no attempts to calculate the KER distributions for highly charged molecular ions. Therefore, in the next chapter we introduce a model which describes the spectra in a semiphenomenological way. Since the scaling with q_1q_2 is inherent in the simple CE model only, we present in Fig. 5 the same results as in Fig. 4(b) but as function of the charge of one of the fragments q_1. The predictions of the simple CE model are also shown by the dashed curves separately for $q_1=q_2$ and for $q_1=q_2+1$. The solid curves present the result of the calculations based on the model described below.

IV. THE AVERAGE BUNCH STATISTICAL MODEL

A. Formulation of the model

For a theoretical description of the KER distribution we suggest a model which is based on a statistical approach and which is semiphenomenological in that it contains adjustable parameters which are to be fitted by comparing the theoretical and experimental distributions.

The model is based on the commonly accepted picture of dissociative ionization by fast ion impact. In the projectile velocity range considered here the collision time ($10^{-17}-10^{-18}$ s) is much shorter than the characteristic time of the nuclear motion in molecules (10^{-13} s) as well as the typical time of dissociation (10^{-14} s). Therefore, we can accept that during the collision the molecule is fixed in space and the internuclear distance remains equal to the equilibrium one (R_e) while a certain number of electrons is removed from the molecule. In addition, due to the fact that the characteristic time of autoionization or Auger decay is 10^{-15} s, some additional number of electrons may be emitted before the dissociation starts. Accordingly, it is usually assumed that the formation of the transient molecular ion in a definite charge state q can be well separated from the dissociation into fragments with charges q_1 and q_2 so that $q=q_1+q_2$.

We consider fast collisions in the case of strong interaction, i.e., $\kappa>1$. In this collision regime the target molecule is strongly perturbed and after losing several electrons the molecular ion is still in a highly excited state [13,17]. Due to the very short collision time which is much shorter than the time of electronic relaxation at least for the valence electrons, the collision may be considered as a sudden perturbation. For the remaining electrons the screening has suddenly changed due to removal of several electrons. Therefore, with high probability they are shaken up to higher orbits, the probability of excitation being distributed among many excited states of the molecular ion. The experimental data confirm this reasoning since it has been observed [18] (see also Fig. 2 in the present paper) that an increase of the interaction strength increases the average excitation energy as well as the width of the KER distributions until, in the strong interaction region, saturation occurs and the width becomes constant.

In principle, it would be possible to calculate the potential curves for all excited states of the molecular ion and calculate the kinetic energy released for each case. The sum over all excitations would then give the KER distribution. There were several attempts to implement such a program, albeit only for a few lowest excited states [2,11,22] (about 60 excited states were considered in a very recent paper [9]). For smaller values of κ and for the lowest degrees of ionization (usually $q=2$) the KER spectra were described successfully. For highly ionized molecules, calculations of the potential energy curves were so far limited to one or a few lowest molecular states [16,25–27]. They qualitatively confirm that the non-Coulombic character of the potential energy curves is important to explain the KER distributions also for high values of q. However, it is clear that for stronger interaction and for higher ionization states the number of excited molecular levels increases enormously. According to calculations [28,29], even for the triply ionized CO molecule more than 300 excited states exist below the threshold for fourfold ionization. Evidently, the direct calculation of all these potential curves would be a formidable and hardly feasible task. On the other hand, the large number of excited states suggests to use some kind of statistical approach, in which some average characteristics are calculated instead of individual potential energy curves. In addition, numerous possible avoided crossings can contribute to the averaging of the contributions of individual potential curves.

Now we describe a simple semiphenomenological model based on the statistical approach. The basic assumptions are the following.

(1) The dense manifold of potential energy curves of the multiply charged molecular ion is represented by a series of similar bunches of potential energy curves correlating with one or several closely lying states of the atomic ions in the dissociation limit (see Fig. 6). In the spirit of the statistical approach we suppose that all molecular states are equally populated in the collision with some average transition probability, the value of which is irrelevant to our consideration of the shape of the KER distribution.

(2) All curves in a bunch are supposed to be of the repul-

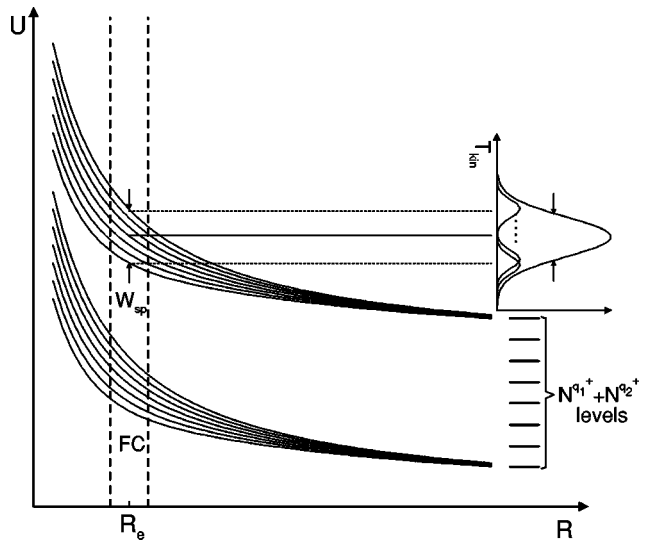

FIG. 6. The formation of the KER distribution in the average bunch statistical model. Two bunches of curves represent schematically the potential energy curves correlated with some excited levels of the ion pair. The dashed vertical lines limit the Franck-Condon region. The formation of the KER spectra is illustrated for one of the bunches in the right part of the figure.

sive type. Therefore, we ignore the so-called quasibound or metastable states which exhibit local minima. This is justified for molecular ions of $q>2$ where the number of such states is negligibly small (see, for example, Ref. [30], and references therein).

(3) As usual, we assume that the collision excites the molecule in the Franck-Condon region (limited by dashed vertical lines in Fig. 6) ''vertically'' from the $\nu=0$ level of the $X\,^1\Sigma^+$ state. Each potential curve of an excited level bunch gives its contribution to the KER distribution as a reflection of the ground state probability density off the repulsive potential energy curve. These individual contributions are narrow and approximately Gaussian-shaped kinetic energy distributions. The total width of the KER distribution is then mainly determined by the spread of the potential energy curves in the bunch taken at the equilibrium distance R_e. Since we assume that all bunches are similar it is sufficient to explicitely consider only one bunch; other bunches give identical contributions which sum up to the total KER distribution.

(4) There may be numerous (avoided) level crossings in the manifold of the potential energy curves. They aid the statistical distribution of the excitation in each bunch but we will ignore their detailed influence on the shape of the KER distribution.

Now we present a more detailed analysis of the potential curve behavior for multicharged molecular ions and discuss various contributions to the width of the KER distributions. Our aim is to estimate the spread of the potential energy curves of one bunch at the internuclear distance around R_e. Consider first two ions A^{q_1+} and B^{q_2+} at the larger distance $R>R_e$ where the overlap of electron clouds may be disregarded. In this case the interaction of two ions can be considered as a perturbation. In the following discussion we closely follow the considerations described in the book by Nikitin and Umanskii [31], adapted to the case of two interacting ions. The molecular terms $U(R)$ may be obtained from the secular equation

$$\mathrm{Det}\langle \gamma_1 \gamma_2 \Gamma \mid H-U \mid \gamma_1' \gamma_2' \Gamma' \rangle = 0. \tag{3}$$

Here γ_1 and γ_2 denote all quantum numbers which are necessary to specify the asymptotic ionic states of A^{q_1+} and B^{q_2+}, respectively, and Γ denotes a set of molecular quantum numbers. Within the framework of the second-order perturbation theory the Hamiltonian of the system may be written as

$$H=H_{0A}+H_{0B}+V_{AB}+V_{AB}^{(2)}+V_{\mathrm{ex}}+V_{\mathrm{SO}}, \tag{4}$$

where H_{0A} and H_{0B} are the Hamiltonians of the ions A and B, V_{AB} is the electrostatic interaction between the two ions, $V_{AB}^{(2)}$ represents the dispersion interaction which for neutral atoms leads to the van der Waals force [superscript (2) indicates that this term gives contribution in the second order perturbation treatment], V_{ex} describes the exchange interaction between the two ions, and V_{SO} is the spin-orbit coupling correction to the nonrelativistic Hamiltonian.

The term $H_{0A}+H_{0B}$ provides the same contribution $\epsilon_{\gamma_1}+\epsilon_{\gamma_2}$ to all diagonal matrix elements in Eq. (3). It can be taken as zero for all molecular terms of the bunch since they converge to the same energy levels of the free ions.

The Coulomb operator V_{AB} can be expanded in multipoles. At large R this expansion can be written in the form [31,32]

$$V_{AB}=\sum_{\kappa_1=0}^{\infty}\sum_{\kappa_2=0}^{\infty} R^{-(\kappa_1+\kappa_2+1)} \sum_{q=-\kappa_{\min}}^{q=\kappa_{\min}} C_{\kappa_1\kappa_2 q} Q_{qA}^{\kappa_1} Q_{-qB}^{\kappa_2}. \tag{5}$$

Here $Q_{qA}^{\kappa_1}, Q_{-qB}^{\kappa_2}$ are the spherical components of the multipole moment operators of ranks κ_1 and κ_2 for the ions A and B, respectively, and $C_{\kappa_1\kappa_2 q}$ are the known coefficients [32]. Due to symmetry considerations for identical ions the summation in Eq. (5) is limited by the condition $\kappa_1+\kappa_2=$ even.

Obviously, the main contribution to V_{AB} comes from the monopole ($\kappa_1=\kappa_2=0$) term which is the usual Coulomb interaction of two pointlike ions: $V_{AB}^0=q_1q_2/R$. If the internuclear distance diminishes, the electronic clouds overlap and the screening of the nuclear charges decreases. At very small distances this part of the interaction is simply Z_AZ_B/R where Z_A and Z_B are the charges of the nuclei. At intermediate distances, the behavior of the potential can be approximated by an appropriate screening function as follows:

$$V_{AB}^0=\frac{Z_AZ_B}{R}\zeta(R)+\frac{q_1q_2}{R}[1-\zeta(R)], \tag{6}$$

where the screening function $\zeta(R)$ has the boundary conditions

$$\zeta(0)=1, \quad \zeta(\infty)=0. \tag{7}$$

In the literature numerous analytical forms of the screening function exist (see, for example, Ref. [33]). We have chosen the simplest exponential form suggested by Bohr [34]

$$\zeta(R)=\exp(-R/a_B), \tag{8}$$

where a_B is the Bohr screening radius which we have slightly modified to account for its decrease with increasing ionic charge

$$a_B=[(Z_A-q_1)^{2/3}+(Z_B-q_2)^{2/3}]^{-1/2}. \tag{9}$$

Now we return to the formulation of our model and add to the four assumptions discussed above the following two assumptions.

(5) We suppose that on average the dependence of the molecular ion potential curves on the internuclear distance is determined by the screened potential (6).

(6) The other potential curves of the bunch are spread around the curve (6). This spread is due to other terms of the Hamiltonian (4), and its value is determined by the average value of the matrix elements

$$W_{\rm sp}\sim M_{\rm av}=\langle \gamma_1\gamma_2\Gamma \mid \tilde{V}_{AB}+V_{AB}^{(2)}+V_{\rm ex}+V_{\rm SO} \mid \gamma_1'\gamma_2'\Gamma'\rangle_{\rm av}, \tag{10}$$

where $\tilde{V}_{AB}=V_{AB}-V_{AB}^0$. We now analyze the contribution of each term in Eq. (10), thereby trying to determine the reason for the steep (approximately quadratic) increase of the spread with the ionic charge.

$V_{\rm SO}$: The spin-orbit interaction increases rapidly with the effective charge ''seen'' by the active electron [35],

$$V_{\rm SO}\sim C_{\rm SO}Z_{\rm eff}^4, \tag{11}$$

where $Z_{\rm eff}$ is some interpolated value lying between the effective charge in the united atom ($R=0$) and in the separated atoms ($R=\infty$) [31]. The constant $C_{\rm SO}$, however, is very small, of the order of 10^{-4} a.u. [35]. One can easily estimate the spin-orbit splitting in molecular ions by comparing it with the splitting of inner atomic shells known from x-ray spectra. The largest value of $Z_{\rm eff}$ in the united atom (Si^{q+}) limit for the outermost electrons at $q=10$ is about 11.8 which approximately corresponds to the effective charge seen by the $2p$ electron in Ti. The corresponding spin-orbit splitting is 6 eV [36]. Comparing this number with the width of the KER distribution which in this case is about 120 eV for $N^{5+}+N^{5+}$ we conclude that the spin-orbit interaction can be simply ignored in our approximate analysis.

$V_{\rm ex}$: The exchange matrix elements can be roughly approximated [31,37] by

$$V_{\rm ex}\sim C_{\rm ex}N_AN_BR^{\xi}\exp(-\mu R), \tag{12}$$

where $C_{\rm ex}$ is a constant of the order of unity which depends on the particular quantum numbers of states; N_A and N_B are the number of active electrons in the ions A and B, respectively, and

$$\xi=\frac{2}{\alpha}+\frac{2}{\beta}-\frac{1}{\mu}-1, \tag{13}$$

$$\mu=\alpha+\beta. \tag{14}$$

In the latter equations α and β are determined by the binding energies ($I_{A(B)}$) or the effective charges ($Z_{{\rm eff},A(B)}$) for the electrons

$$\alpha=(2I_A)^{1/2}\simeq Z_{{\rm eff},A}/n_A, \tag{15}$$

$$\beta=(2I_B)^{1/2}\simeq Z_{{\rm eff},B}/n_B, \tag{16}$$

where n_A and n_B are the principal quantum numbers of active electrons (in our case $n_{A(B)}=2$). For a rough estimate we can put $Z_{{\rm eff},A}=q_1+1$; $Z_{{\rm eff},B}=q_2+1$. A simple calculation using Eqs (12)–(16) shows that at the distance R_e the value of matrix elements $V_{\rm ex}$ becomes negligible for $q>3$ mainly due to the exponential factor $\exp(-\mu R)$. Therefore, we ignore the exchange contribution in the further analysis.

$\tilde{V}_{AB}$: An important contribution can come from the Coulomb interaction. The leading term in the expansion (5) which can contribute to the spreading width is the monopole-quadrupole term which can be expressed as

$$\tilde{V}_{AB}\simeq C_{AB}\frac{q_1\langle Q_B^2\rangle+q_2\langle Q_A^2\rangle}{R^3+R_c^3}. \tag{17}$$

Here C_{AB} is a constant of the order of unity which depends on the quantum numbers of the states considered and $\langle Q_{A(B)}^2\rangle$ are the quadrupole moments. As usual, in Eq. (17) we have introduced a cutoff radius $R_c\simeq 2$ a.u. [31,38] in order to remove an unrealistic dominance of this term at small separations. To estimate the quadrupole moments we note that

$$\langle Q_{A(B)}^2\rangle\sim N_{A(B)}\langle r^2\rangle\sim N_{A(B)}/Z_{{\rm eff},A(B)}^2\simeq N_{A(B)}/(q_{1(2)}+1)^2, \tag{18}$$

where $\langle r^2\rangle$ is the mean square radius of the electron distribution. Substituting Eq. (18) into Eq. (17) we obtain an estimate of the contribution of the Coulomb interaction $\tilde{V}_{AB}$.[1] It contributes considerably to the spreading width of the bunch. However, as can be easily seen from Eqs. (17), (18), it is diminishing with an increase of ionicity q and thus cannot alone explain the observed increase of the KER distribution width at large q.

$V_{AB}^{(2)}$: Finally, consider the dispersion (second order) interaction which originates from the mutual polarization of the ions. Due to the ionic charge, the lowest order term in a R^{-1} expansion is R^{-4}. It is usually written [38] as

$$V_{AB}^{(2)}=C_{\rm disp}\frac{q_1^2\alpha_B+q_2^2\alpha_A}{2(R^2+R_c^2)^2}, \tag{19}$$

[1]We note that a similar contribution with the same R dependence will be given by the dipole-dipole interaction. This interaction contributes to first-order perturbation theory only when the basis set involves pairs of atomic states of different parity. For simplicity we ignore this term.

where $\alpha_{A(B)}$ is the dipole polarizability of the corresponding ion, $C_{\rm disp}$ is a constant of the order of unity which depends on the quantum numbers of ionic states, and R_c is the cutoff radius which we choose to be the same as above. The dipole polarizability of the ions can be estimated by the empirical relation suggested in Ref. [37,39]. Using this expression we obtain values of $\alpha_{A(B)}$ in the range $3.4-2.5$ a.u. for nitrogen ions with $q_{1(2)}=2-4$. The polarizability slowly decreases with increasing ion charge. However, we should take into account that this empirical expression applies to the ionic ground state while we discuss the excited states where the polarizability may be larger. Having this in mind and trying not to unnecessarily increase the number of unknown parameters we assume the polarizability to be approximately independent of q. In this case the only adjustable parameter is the product $C_{\rm disp}\alpha_{A(B)}$. Inspecting now expression (19) we see that it has quadratic dependence on the ion charge; therefore it provides the necessary increase of the spreading of the molecular terms with increase of the total ion charge.

Summarizing this analysis we conclude that the most important contribution to the spread of the potential curves of one particular bunch comes from the Coulomb interaction and the dispersion interaction. The former is more important for the low-charge ions ($q=4-6$) while the latter is more important for the higher charges $q=6-10$. Expressions (17) and (19) contain two adjustable parameters, C_{AB} and $C_{\rm disp}$ (or $C_{\rm disp}\alpha_{A(B)}$), which may be varied to achieve agreement with the experiment.

B. Model calculations and comparison with the experimental data

We calculate the model KER distribution assuming the molecular states to be randomly distributed within a particular bunch; we describe their density by a Gaussian distribution with its maximum value at the energy determined by $V^0_{AB}(R_e)$ [see Eq. (6)]. The level dispersion is given by

$$W_{sp}=\tilde{V}_{AB}(R_e)+V^{(2)}_{AB}(R_e), \tag{20}$$

with $\tilde{V}_{AB}(R_e)$ and $V^{(2)}_{AB}(R_e)$ from Eqs. (17) and (19), respectively. For each of the potential energy curves the KER is then calculated using the reflection method. The total KER distribution is obtained by summation of the partial distributions.

The fitting parameters are chosen to be $C_{AB}=1.2$ and $C_{\rm disp}\alpha_{A(B)}=6.2$. The latter value yields $C_{\rm disp}=1.6-2$ for a dipole polarizability of about $3-4$ a.u. (see above). The results of the calculations are shown in Figs. 1,4,5. The calculated most probable KER and the FWHM for each of the KER distributions are presented in Figs. 4 and 5. Evidently, the model calculations can satisfactorily reproduce not only the position of the experimental maximum but also the width of the KER distributions.

The resulting KER distributions are slightly asymmetric of approximately Gaussian shape. For some cases they are compared with the experimental spectra in Fig. 1. We see that the overall agreement is quite good.

V. CONCLUDING REMARKS

We have presented experimental results for the distributions of the total kinetic energy of multicharged fragments produced in collisions of N_2 molecules with fast highly charged Xe and Bi ions. We have observed that in the strong interaction region ($\kappa>2-3$) the KER spectra are practically independent of the projectile charge and velocity. The spectra for large $q>3$ have a simple shape without any pronounced structure. Striking similarity is found for the KER distributions of ion pairs which correspond to different dissociation channels of one and the same parent molecular ion, indicating a strong interchannel interaction during dissociation. We have also found that the width of the KER distributions increases rapidly with the transient molecular ion charge, reaching a value of about $100-120$ eV for $q\sim 10$. The CE model for point charges fails to explain such a large width although it predicts the position of the KER maximum fairly well.

We have developed a more elaborate semiphenomenological model which describes the dissociation of a highly excited multicharged molecular ion. With this model we are able to reproduce both the position and the width of the observed spectra. The model implies that the rapid increase of the width of KER distributions is connected with the spread of the potential energy curves due to the mutual polarization of the molecular fragments. The model may be applied to other diatomics and, probably, more complex molecules. To test its validity it would be of interest to measure the Coulomb fragmentation of heavier diatomics as, for example, Br_2 or I_2, where one could expect even larger widths of KER distributions due to the larger polarizability of these molecules. Such experiments are under consideration.

ACKNOWLEDGMENTS

The authors wish to thank the GSI staff for their hospitality and their support during the measurements. We are indebted to J. Hinze for stimulating discussions and useful comments. N.M.K. is grateful to Bielefeld University for hospitality. This work has been supported in part by the Deutsche Forschungsgemeindshaft (DFG) in the project ''Strahlungswechselwirkungen,'' by the EU Infrastructure Cooperation Network No. HRPI-1999-4009, and by the Gesellschaft für Schwerionenforschung in the project BILUTA.

[1] C. J. Latimer, Adv. At. Mol., Opt. Phys. **30**, 105 (1993).
[2] U. Werner, K. Beckord, J. Becker, H. O. Folkerts, and H. O. Lutz, Nucl. Instrum. Methods Phys. Res. B **98**, 385 (1995).
[3] H. O. Folkerts, R. Hoekstra, and R. Morgenstern, Phys. Rev. Lett. **77**, 3339 (1996).
[4] U. Werner, J. Becker, T. Farr, and H. O. Lutz, Nucl. Instrum. Methods Phys. Res. B **124**, 298 (1997).
[5] H. O. Folkerts, F. W. Bliek, M. C. de Jong, R. Hoekstra, and R. Morgenstern, J. Phys. B **30**, 5833 (1997).
[6] H. O. Folkerts, T. Schlathölter, R. Hoekstra, and R. Morgen-

stern, J. Phys. B **30**, 5849 (1997).
[7] K. F. Dunn, P. A. Hatherly, C. J. Latimer, M. B. Shah, C. Browne, A. M. Sands, B. O. Fisher, M. K. Thomas, and K. Codling, *Application of Accelerators in Research and Industry*, edited by J. L. Duggan and J. L. Morgan, AIP Conf. Proc. No. 475 (AIP, Woodbury, NY, 1999), p. 162.
[8] R. D. DuBous, T. Schlathölter, O. Hadjar, R. Hoekstra, R. Morgenstern, C. M. Doudna, R. Feeler, and R. E. Olson, Europhys. Lett. **49**, 41 (2000).
[9] M. Tarisien, L. Adoui, F. Frémont, D. Lelièvre, L. Guillaume, J.-Y. Chesnel, H. Zhang, A. Dubois, D. Mathur, S. Kumar, M. Krishnamurthy, and A. Cassimi, J. Phys. B **33**, L11 (2000).
[10] U. Werner, K. Beckord, J. Becker, and H. O. Lutz, Phys. Rev. Lett. **74**, 1962 (1995).
[11] B. Siegmann, U. Werner, and H. O. Lutz, Aust. J. Phys. **52**, 545 (1999).
[12] A. K. Edwards and R. M. Wood, J. Chem. Phys. **76**, 2938 (1982).
[13] G. Sampoll, R. L. Watwon, O. Heber, V. Horvat, K. Wohrer, and M. Chabot, Phys. Rev. A **45**, 2903 (1992).
[14] I. Ben-Itzhak, S. G. Ginther, and K. D. Carnes, Phys. Rev. A **47**, 2827 (1993).
[15] I. Ben-Itzhak, K. D. Carnes, S. G. Ginther, D. T. Johnson, P. J. Norris, and O. L. Weaver, Phys. Rev. A **47**, 3748 (1993).
[16] D. Mathur, E. Krishnakumar, K. Nagesha, V. R. Marathe, V. Krishnamurthi, F. A. Rajara, and U. T. Raheja, J. Phys. B **26**, L141 (1993).
[17] I. Ben-Itzhak, S. G. Ginther, V. Krishnamurthi, and K. D. Carnes, Phys. Rev. A **51**, 391 (1995).
[18] V. Krishnamurthi, I. Ben-Itzhak, and K. D. Carnes, J. Phys. B **29**, 287 (1996).
[19] R. L. Watson, G. Sampoli, V. Horvat, and O. Heber, Phys. Rev. A **53**, 1187 (1996).
[20] L. Adoui, C. Caraby, A. Cassimi, D. Lelièvre, J. P. Grandin, and A. Dubois, J. Phys. B **32**, 631 (1999).
[21] U. Brinkmann, A. Reinköster, B. Siegmann, U. Werner, H. O. Lutz, and R. Mann, Phys. Scr. **T80**, 171 (1999).
[22] B. Siegmann, U. Werner, U. Brinkmann, A. Reinköster, C. Haumann, H. O. Lutz, and R. Mann, J. Phys. B (to be published).
[23] J. Becker, K. Beckord, U. Werner, and H. O. Lutz, Nucl. Instrum. Methods Phys. Res. A **337**, 409 (1994).
[24] R. Moshammer, M. Unverzagt, W. Schmitt, J. Ullrich, and H. Schmidt-Böcking, Nucl. Instrum. Methods Phys. Res. B **108**, 425 (1996).
[25] H. Hartung, B. Fricke, T. Morovic, and W. D. Sepp, Phys. Lett. **69A**, 87 (1978).
[26] A. Remscheid, B. A. Huber, M. Pykavyj, V. Staemmler, and K. Wiesemann, J. Phys. B **29**, 515 (1996).
[27] J. S. Wright, G. A. DiLabio, D. R. Matusek, P. B. Corkum, M. Yu. Ivanov, Ch. Ellert, R. J. Buenker, A. B. Alekseyev, and G. Hirsch, Phys. Rev. A **59**, 4512 (1999).
[28] G. Handke, F. Tarantelli, A. Sgamellotti, and L. S. Cederbaum, J. Electron Spectrosc. Relat. Phenom. **76**, 307 (1995).
[29] G. Handke, F. Tarantelli, and L. S. Cederbaum, Phys. Rev. Lett. **76**, 896 (1996).
[30] P. J. Bruna and J. S. Wright, J. Phys. B **26**, 1819 (1993).
[31] E. E. Nikitin and S. Ya. Umanskii, *Theory of Slow Atomic Collisions* (Springer-Verlag, Berlin, 1984).
[32] C. G. Gray, Can. J. Phys. **46**, 135 (1968).
[33] I. M. Torrens, *Interatomic Potentials* (Academic Press, New York, 1972).
[34] N. Bohr, K. Dan. Vidensk. Selsk. Mat. Fys. Medd. **18**, 8 (1948).
[35] I. I. Sobel'man, *Introduction to the Theory of Atomic Spectra* (Pergamon Press, Oxford, 1972).
[36] J. A. Bearden and A. F. Burr, Rev. Mod. Phys. **39**, 125 (1967).
[37] V. G. Pal'chikov and V. P. Shevelko, *Reference Data on Multicharged Ions* (Springer-Verlag, Berlin, 1995).
[38] C. Laughlin and G. A. Victor, Adv. At. Mol. Phys. **25**, 163 (1988).
[39] A. D. Ulantsev and V. P. Shevelko, Opt. Spectrosc. **65**, 590 (1988).